Geophysical Research Letters

RESEARCH LETTER
10.1029/2018GL078356

Key Points:
- The steady state stress exponent of ice in polar ice sheets is approximately four
- Underestimating the stress exponent causes an overestimate of basal motion
- The proposed stress exponent significantly reduces basal motion and therefore assumed basal thawing in polar ice sheets

Supporting Information:
- Supporting Information S1
- Data Set S1

Correspondence to:
P. D. Bons,
paul.bons@uni-tuebingen.de

Citation:
Bons, P. D., Kleiner, T., Llorens, M.-G., Prior, D. J., Sachau, T., Weikusat, I., & Jansen, D. (2018). Greenland Ice Sheet: Higher nonlinearity of ice flow significantly reduces estimated basal motion. *Geophysical Research Letters*, *45*, 6542–6548. https://doi.org/10.1029/2018GL078356

Received 14 APR 2018
Accepted 7 JUN 2018
Accepted article online 19 JUN 2018
Published online 5 JUL 2018

Greenland Ice Sheet: Higher Nonlinearity of Ice Flow Significantly Reduces Estimated Basal Motion

P. D. Bons[1], T. Kleiner[2], M.-G. Llorens[1,3], D. J. Prior[4], T. Sachau[1], I. Weikusat[1,2], and D. Jansen[2]

[1]Department of Geosciences, Eberhard Karls University Tübingen, Tübingen, Germany, [2]Alfred Wegener Institute Helmholtz Centre for Polar and Marine Research, Bremerhaven, Germany, [3]Departament de Geologia, Universitat Autònoma de Barcelona, Barcelona, Spain, [4]Department of Geology, University of Otago, Dunedin, New Zealand

Abstract In times of warming in polar regions, the prediction of ice sheet discharge is of utmost importance to society, because of its impact on sea level rise. In simulations the flow rate of ice is usually implemented as proportional to the differential stress to the power of the exponent $n = 3$. This exponent influences the softness of the modeled ice, as higher values would produce faster flow under equal stress. We show that the stress exponent, which best fits the observed state of the Greenland Ice Sheet, equals $n = 4$. Our results, which are not dependent on a possible basal sliding component of flow, indicate that most of the interior northern ice sheet is currently frozen to bedrock, except for the large ice streams and marginal ice.

Plain Language Summary Ice in the polar ice sheets flows toward the oceans under its own weight. Knowing how fast the ice flows is of crucial importance to predict future sea level rise. The flow has two components: (1) internal shearing flow of ice and (2) basal motion, which is sliding along the base of ice sheets, especially when the ice melts at this base. To determine the first component, we need to know how *soft* the ice is. By considering the flow velocities at the surface of the northern Greenland Ice Sheet and calculating the stresses that cause the flow, we determined that the ice is effectively softer than is usually assumed. Previous studies indicated that the base of the ice is thawed in large parts (up to about 50%) of the Greenland Ice Sheet. Our study shows that that is probably overestimated, because these studies assumed ice to be harder than it actually is. Our new assessment reduces the area with basal motion and thus melting to about 6–13% in the Greenland study area.

1. Introduction

Ice is constantly transported from ice sheets to the surrounding oceans by gravity-driven flow. The flow velocity of ice is assumed to have two main components. First, ice exhibits crystal-plastic behavior that leads to nonlinear viscous flow (Budd & Jacka, 1989; Durham et al., 1983; Glen, 1952, 1955; Goldsby & Kohlstedt, 2001; Hutter, 1983; Treverrow et al., 2012; Weertman, 1983). The second is *basal motion* due to sliding over the bedrock or shearing within subglacial sediments, when the base is thawed (Bell et al., 2014; Fahnestock et al., 2001; Hewitt, 2013; MacGregor et al., 2016; Rignot & Mouginot, 2012; Sergienko et al., 2014; Stokes et al., 2007; Wolovick et al., 2014). Recent studies have proposed that basal motion may dominate ice transport in up to 50% of the Greenland ice sheet area (Rignot & Mouginot, 2012); MacGregor et al., 2016). These studies used measurements of surface velocities in combination with inverse modeling, to determine the contribution of each of the two velocity components to the total ice transport rate. An underestimate of the internal deformation rate of the ice automatically leads to an overestimate of the basal motion. A correct description of the ice flow law is therefore crucial to understand current ice transport rates and predict their possible future changes (Clark et al., 2016; Gillet-Chaulet et al., 2012; Graversen et al., 2011; Intergovernmental Panel on Climate Change, 2014; Ren et al., 2011).

Experiments and observations on ice sheets and glaciers suggest that the quasi-viscous rheology of ice can be described with a power law, also known as Glen's law (Glen, 1952, 1955), of the form:

$$\dot{\varepsilon} = A\sigma^n \tag{1}$$

with $\dot{\varepsilon}$ the strain rate, σ the differential stress, n the stress exponent, and A the temperature-dependent rate factor. Stress exponents in the range from one to five are obtained from observations on natural ice flows (borehole deformation measurements, ice flow velocities, etc.; Cuffey & Kavanaugh, 2011; Gillet-Chaulet

et al., 2011; Hutter, 1983; Pettit & Waddington, 2003) and laboratory experiments on polycrystalline ice aggregates at stresses mostly below 1 MPa, as is typical for ice sheets (Durham et al., 1983; Glen, 1955; Goldsby & Kohlstedt, 2001; Hooke, 1981; Treverrow et al., 2012; Weertman, 1983). Although the exact value of the stress exponent of ice under Earth conditions is far from certain, the current literature almost invariably assumes that $n = 3$. Here we reassess and challenge the paradigmatic assumption that $n = 3$ by determining n in situ in the northern Greenland Ice Sheet (GrIS).

2. Materials and Methods

The surface velocity (v_s) of an ice sheet is the sum of v_{ice}, caused by bedrock-parallel shearing inside the ice, and v_{base} due to basal motion. We use the Shallow Ice Approximation (SIA; Budd & Jacka, 1989; Hutter, 1983), which ignores all stresses other than the shear stresses resolved on planes parallel to the bedrock. This is valid in areas where all other stress components are small (Kirchner et al., 2016). The advantage of using the SIA here is that no assumptions need to be made on far-field stresses. Measurements obtained from one point on the ice sheet are thus independent of such assumptions. v_{ice} can be related to the driving stress (τ) with

$$v_{ice} = \frac{2A}{n+1} H \tau^n. \tag{2}$$

The driving stress is proportional to the surface gradient (∇S) and local ice sheet thickness (H), according to

$$\tau = -\rho g H \nabla S, \tag{3}$$

with ρ the ice density of 917 kg/m^3 and g the 9.81 m/s^2 gravitational acceleration. Several studies have used this approach, with the a priori assumption that $n = 3$ in Glen's law, to determine the amount of basal motion (MacGregor et al., 2016) and/or the rate factor A (Rignot & Mouginot, 2012). We use the same approach here, but instead, we determine the stress exponent for an area that covers most of the north of GrIS (Figure 1a).

3. Data

We used surface and bedrock elevation data (Bamber et al., 2013) on a rectangular 500-m resolution grid, to determine ice sheet thickness H and surface elevation S for every grid point in the northern part of Greenland. Data analysis was restricted to areas where $H > 200$ m. As the SIA is only an appropriate approximation of the stress state in the ice sheet away from the fast-flowing ice streams, the ice sheet margins and divides (Kirchner et al., 2016), we only take into account data from areas away from these (except for divides, which are discussed below). The driving stress (τ) was obtained from the surface gradient, using equation (3) (Figure 1b). Absolute surface velocities (v_s) and directions of surface flow were obtained from the MEaSUREs velocity data set (Joughin et al., 2010a, 2010b) with data from the years 2000–2008. The surface elevation of GrIS shows undulations and, hence, variations in surface slope, on the 5- to 20-km scale (Sergienko et al., 2014). Surface roughness was removed with a low-pass filter applied to the surface elevation data. After considering several cutoff wavelengths, we found that a 20-km low-pass filter gives the optimal compromise between spatial resolution and data quality, with a smooth distribution of τ (Figures 1b and 2) and a good alignment of the directions of observed surface velocities v_s and τ, except near divides (Figure S1b in the supporting information). The alignment is a prerequisite for the validity of equation (2). Furthermore, 20 km is about 10 times the ice sheet thickness, at which distance longitudinal stresses are eliminated, making the SIA an appropriate approach (Kamb & Echelmeyer, 1986).

4. Results and Discussion

From equation (2) it follows that

$$\log\left(\frac{v_s}{H}\right) = n \log(\tau) + C \text{ with } C = \log\left(\frac{2A}{n+1} + \frac{v_{base}}{H\tau^n}\right) \tag{4}$$

Thus, a double logarithmic plot of the ratio v_s/H and the driving stress τ can be used to determine the stress exponent n from a linear regression. This double logarithmic plot now shows a good correlation (Figure 3).

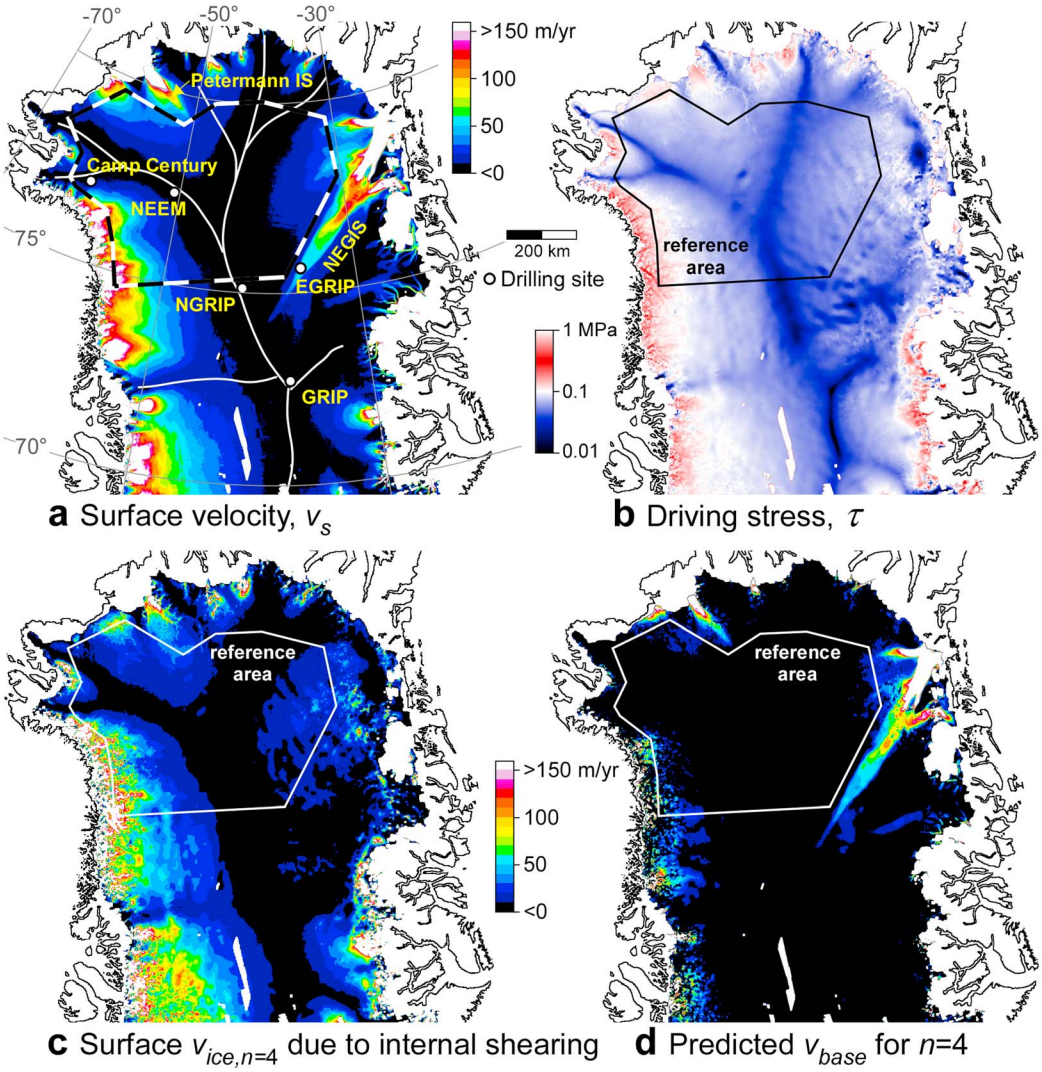

Figure 1. Results of the analysis for the northern Greenland Ice Sheet. (a) Map of northern Greenland showing the surface velocity (v_s) distribution, the main ice streams and deep drilling sites, and the outline of the reference area. (b) Map of the driving stress (τ in MPa) calculated with equation (3), using surface elevation data that were subjected to a 20-km low-pass filter. (c) Map of the surface velocity component ($v_{\mathrm{ice},n=4}$), caused by internal shearing of the ice, calculated with the new $n = 4$ flow law. (d) Predicted basal velocity, calculated by subtracting $v_{\mathrm{ice},n=4}$ from v_s.

Scatter in the v_s/H data can in part be explained by noise and errors in the velocity and bedrock elevation data. With a noise in the order of ±1 m/year in the velocity data, errors are in the order of ±15% at $\tau = 0.05$ MPa, but lower at higher τ. The stress exponent (n) was determined from v_s/H and τ data in a 328,162-km^2 reference area (Figure 1a). A value of $n = 4.10$ was obtained from linear regression of the data points on the log (v_s/H) versus log (τ) graph (Figure 3), for points where $\tau > 0.04$ MPa (87% of the reference area). The regression gives a standard error of $r^2 = 0.925$ and 95% bootstrapped confidence limits at 4.04 and 4.14.

Assuming $n = 4$ and no basal motion, log (A') was calculated for each data point with log (A') = log (v_s/H)-4τ. The flow factor $A_{n=4}$ for $n = 4$ was then obtained by averaging all A' values and using $A_{n=4}=\langle A' \rangle \cdot (n+1)/2$ (based on equation (2)). The rate factor thus obtained for the reference area is $A_{n=4} = 3.3 \cdot 10^{-5}$ MPa^{-4} s^{-1}. As with the published $A_{n=3} = 1.2 \cdot 10^{-6}$ MPa^{-3} s^{-1} for GrIS of Rignot and Mouginot (2012), this is an average rate factor for the whole ice sheet region under consideration.

The flow factor A is a function of a number of state variables, such as lattice preferred orientation (Faria et al., 2014; Graham et al., 2018; Treverrow et al., 2012), grain size (de Bresser et al., 2001; Platt & Behr, 2011),

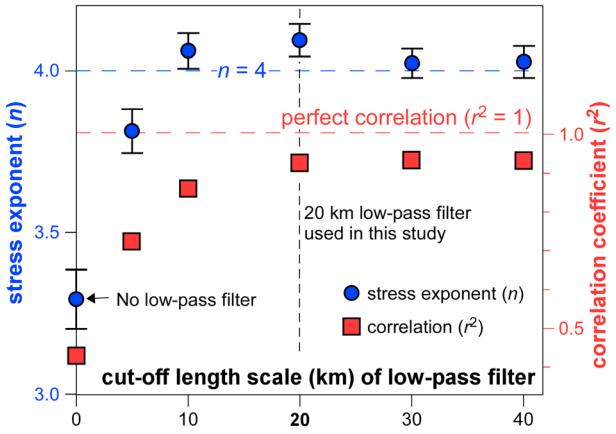

Figure 2. Effect of the choice of low-pass filter on the linear regression of the logarithms of the mean vertical shear strain rate (v_s/H) *versus* the driving stress (τ) data. Blue circles: Stress exponent (n) with error bars representing the 95% bootstrapped confidence intervals. Red squares: Correlation coefficient (r^2).

impurity content (Faria et al., 2009; Paterson, 1991), and temperature. The data plotted in Figure 3 are sampled over a large reference area in which one or more of these variables may potentially vary systematically with τ. If this variation correlates with τ, the slope in the v_s/H versus τ plot would change and an *apparent n-value* would be obtained. It has been argued that glacial ice is softer than Holocene ice, due to the difference in impurity content (Faria et al., 2009; Paterson, 1991). The relative proportion of glacial ice decreases from the divides toward the margins (MacGregor et al., 2015). This would imply a negative correlation between A and τ and would actually lower the apparent n. Basal temperature is expected to increase, lattice preferred orientation to strengthen, and grain size to decrease with increasing τ toward the margins. Unfortunately, it is not known by how much, because very few direct measurements are available as most drill holes were sunk on divides or close to the ice sheet margin. It would be highly coincidental if the variation in these variables would correlate with τ to raise the slope in Figure 3 from the usually assumed n = 3 to exactly four over a large area in the ice sheet. We therefore assume that the observed slope in Figure 3 reflects the stress exponent to be used in the flow law (equation (1)).

It is of interest to note that Glen (1955) himself wrote "... it is noteworthy that practically observable long-time creep rates, as in a glacier, would probably depend on a higher power of the stress than the 3.2 found here." One should note that Glen's law is typically based on the stress/strain rate points from the minimum strain rate or peak/yield stress (Budd & Jacka, 1989; Glen, 1955), rather than those corresponding to steady state flow or tertiary creep. Glen (1955) derives a strain rate minimum n value of 3.2 and shows (Figure 12 in Glen, 1955) data for *quasi-viscous* creep rate that give n = 4. More recent experiments (Qi et al., 2017; Treverrow et al., 2012) give a peak stress (=minimum strain rate) n value of ~3, but a steady state flow stress n value closer to 4, consistent with the n = 4 flow law derived by Durham et al. (1983) and Azuma and Higashi (1984). Considering the high finite strains prevalent in ice sheets, the use of steady state flow data appears to be more appropriate, as is corroborated by our in situ determination of n = 4. Another factor may be that an apparent n = 3 could result from erroneously fitting a stress exponent to data that have been derived in the stress range at the transition between the dislocation creep regime (n = 4) and the regime of basal dislocation glide accompanying grain-boundary sliding (n = 1.8; Goldsby & Kohlstedt, 2001). The good correlation between the ratio v_s/H and the driving stress τ that gives n = 4 breaks down at low τ, which is mostly the case at divides. First, the SIA model does not apply at domes and divides, because flattening stresses cannot be ignored here (Kirchner et al., 2016; Raymond, 1983). This leads to faster flow than predicted by the SIA model and deviating flow directions (Figure S1). Second, grain size-sensitive creep mechanisms may contribute significantly to flow at low stresses, reducing the stress exponent (Goldsby, 2006; Goldsby & Kohlstedt, 2001; Pettit & Waddington, 2003). The transition to this low-stress regime has been proposed to range from 0.02 to 0.05 MPa (Budd & Jacka, 1989; Pettit & Waddington, 2003). Our data suggest that n = 4 applies to driving stresses above about 0.04 MPa (Figure 3), which is in agreement with the aforementioned studies.

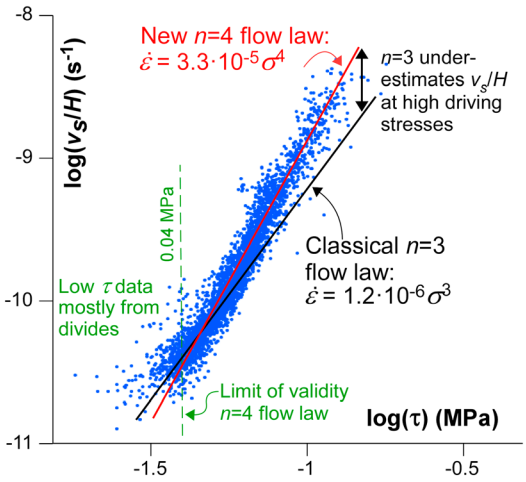

Figure 3. Log (v_s/H) *versus* log (τ) based on data in the reference area. The classical n = 3 flow law (Rignot & Mouginot, 2012) and our new best fit flow law with n = 4 are shown (see supporting information data set DS01 for the raw data).

The choice of the stress exponent is of utmost importance in determining the amount of basal motion in Greenland's ice sheet. A stress exponent that is too low leads to an overestimate of the viscosity at high driving stresses and, therefore, an underestimate of the internal deformation velocity v_{ice}. This in turn leads to an overestimate of the basal velocity, v_{base}. Using the same approach as Rignot and Mouginot (2012) and MacGregor et al. (2016), we mapped the ratio and difference of the actual v_s and the one predicted with the measured n = 4 flow law ($v_{ice,n=4}$) for internal shearing of the ice only (Figures 1c and 1d). Basal

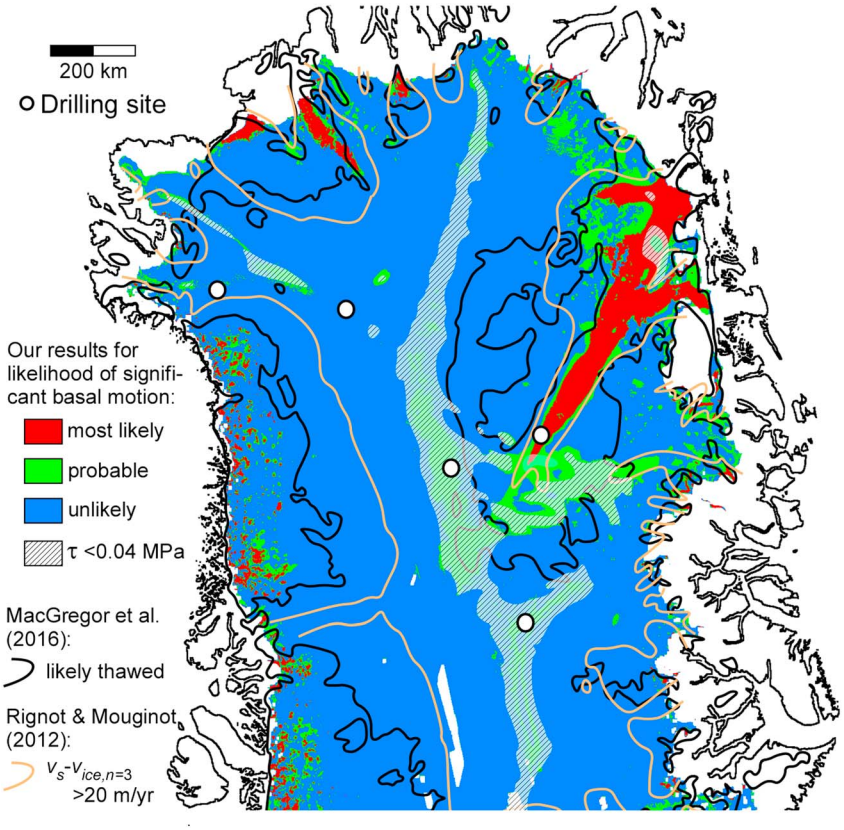

Figure 4. Distribution of the likelihood of basal motion. We use two criteria: (i) the surface velocity (v_s) is more than double the predicted basal velocity (v_{base}) and (ii) v_s minus v_{base} exceeds 20 m/year. Basal motion is *most likely* when both criteria apply, and *probable* when one of two applies. Areas deemed *likely thawed* by MacGregor et al. (2016) and areas where v_s exceeds the velocity predicted by the $n = 3$ flow law ($v_{ice,n=3}$) by ≥20 m/year according to Rignot and Mouginot (2012) are much larger than predicted by our $n = 4$ flow law. Areas where the driving stress is less than 0.04 MPa are shown with dashes.

motion is most likely in areas where the ratio $v_s/v_{ice,n=4}$ exceeds two (the $n = 4$ law accounts for <50% of the actual surface velocity) and where the actual surface velocity exceeds $v_{ice,n=4}$ by ≥20 m/year (Rignot & Mouginot, 2012; Figure 4). Both indicators for basal motion are fulfilled in ~6% of the northern GrIS area where $\tau > 0.04$ MPa, while only one of the two criteria is fulfilled in another ~7%. Enhanced velocities are found at the margins of the ice sheet and at ice streams. The enhanced velocities (most distinct in Northeast Greenland Ice Stream (NEGIS)) are clear indications for an additional transport mechanism, most probably basal motion due to a thawed base (Fahnestock et al., 2001). However, the use of $n = 4$ significantly reduces the area with significant basal motion compared to current estimates that are based on an $n = 3$ rheology (MacGregor et al., 2016; Rignot & Mouginot, 2012).

When calculating the mismatch between observed velocities and calculated velocities with $n = 4$, our results indicate that the base of the ice may be thawed at the location of NorthGrip (Dahl-Jensen et al., 2003; but note that $\tau < 0.04$; Figure 4). NorthGrip lies in the west of a large area that includes the onset of NEGIS and where large patches of basal melting are indicated, consistent with enhanced geothermal heat flow in this region (Fahnestock et al., 2001; Rogozhina et al., 2016).

5. Conclusions

A stress exponent of four has now been determined in situ, for the first time in a large area in an ice sheet, consistent with experimental data that use the flow or steady strain rate/stress (Durham et al., 1983; Qi et al., 2017; Treverrow et al., 2012) rather than the strain rate minimum or peak stress and in situ measurements on much smaller areas (Gillet-Chaulet et al., 2011). Above, we highlighted the implications of a higher n than commonly assumed on estimates of the amount of basal motion in the northern part of GrIS. Since the

stress exponent is a material property of ice, this observation is not restricted to GrIS but also applicable to the Antarctic Ice Sheet and mountain glaciers. However, the implications reach much further. (i) Strong, centimeter-scale flow heterogeneity in ice is observed in numerical simulations of ice deformation (Llorens et al., 2016; using $n = 3$) and disturbances in layering in ice cores (Jansen et al., 2016). Our unpublished simulations show that the heterogeneity increases when n is raised and extends to all scales, as is observed in rocks (Carreras, 2001; de Riese et al., 2018). (ii) Overestimating basal motion can lead to misinterpretations of the cause for large-scale folding observed in radar stratigraphy (compare Wolovick et al., 2014, and Bons et al., 2016). (iii) The vertical-velocity profile depends on n. As a consequence, the total mass flux at a given surface velocity and ice thickness is about 5% higher for $n = 4$ compared to $n = 3$. Models that use $n = 3$ (Gillet-Chaulet et al., 2012; Graversen et al., 2011; Karlsson & Dahl-Jensen, 2015; Ren et al., 2011) may thus underestimate ice fluxes or may compensate for this by invoking basal motion. Increasing n also reduces the kink-point height h in the velocity profile that is used in the Dansgaard-Johnsen model to predict age-depth relationships (Dansgaard & Johnsen, 1969). This has implications for inferences on the amount of basal melting based on measurements of h (e.g., Fahnestock et al., 2001; MacGregor et al., 2016). (iv) The even stronger nonlinearity with $n = 4$ means that the ice sheet is responding faster to changes in boundary conditions, which also means that changing and retreating grounding lines can affect the flux of inland ice in shorter times (Gillet-Chaulet et al., 2011). It remains to be determined whether these implications in combination make ice sheets less or more stable under changing conditions. What can be inferred is that the internal deformation of ice plays a bigger role than hitherto assumed. Considering the importance of correctly predicting ice sheet behavior and related sea level rise, with results of models feeding into global political-economical decisions, it is imperative that ice flow modelers start considering $n = 4$, at least as an alternative to only $n = 3$.

Acknowledgments

This research was funded by HGF-grant VH-NG-802 to D. J. and I. W. M. G. L. was funded by the programme for Recruitment of Excellent Researchers of the Eberhard Karls University Tübingen. We thank Nobuhiko Azuma and Ed Waddington for their careful reviews. Surface and bedrock elevation data were kindly provided by J. L. Bamber. An older, lower-resolution data set can be obtained from NSIDC (http://nsidc.org/data/nsidc-0092). Surface velocities (Joughin et al., 2010a, 2010b) can be obtained from NSIDC (http://nsidc.org/data/NSIDC-0670). Derived data are available from the PANGAEA repository at https://doi.pangaea.de/10.1594/PANGAEA.890558 (doi: 10.1594/PANGAEA.890558). These are maps of the surface elevation (S), ice thickness (H), driving stress, the v_s/H ratio, predicted surface velocity for $n = 4$ (v_{ice}), and the predicted basal velocity for $n = 4$ (v_{base}). Data plotted in Figure are provided as supporting information Data Set S1.

References

Azuma, N., & Higashi, A. (1984). Mechanical properties of Dye 3 Greenland deep ice cores. *Annals of Glaciology*, *5*, 1–8. https://doi.org/10.3189/1984AoG5-1-1-8

Bamber, J. L., Griggs, J. A., Hurkmans, R. T. W. L., Dowdeswell, J. A., Gogineni, S. P., Howat, I., et al. (2013). A new bed elevation dataset for Greenland. *The Cryosphere*, *7*(2), 499–510. https://doi.org/10.5194/tc-7-499-2013

Bell, R. E., Tinto, K., Das, I., Wolovick, M., Chu, W., Creyts, T. T., et al. (2014). Deformation, warming and softening of Greenland's ice by refreezing meltwater. *Nature Geoscience*, *7*, 497–502. https://doi.org/10.1038/ngeo2179

Bons, P. D., Jansen, D., Mundel, F., Bauer, C. C., Binder, T., Eisen, O., et al. (2016). Converging flow and anisotropy cause large-scale folding in Greenland's ice sheet. *Nature Communications*, *7*, 11427. https://doi.org/10.1038/ncomms11427

Budd, W. F., & Jacka, T. H. (1989). A review of ice rheology for ice sheet modeling. *Cold Regions Science and Technology*, *16*, 107–144.

Carreras, J. (2001). Zooming on Northern Cap de Creus shear zones. *Journal of Structural Geology*, *23*, 1457–1486. https://doi.org/10.1016/S0191-8141(01)00011-6

Clark, P. U., Shakun, J. D., Marcott, S. A., Mix, A. C., Eby, M., Kulp, S., et al. (2016). Consequences of twenty-first-century policy for multi-millennial climate and sea-level change. *Nature Climate Change*, *6*(4), 360–369. https://doi.org/10.1038/nclimate2923

Cuffey, K. M., & Kavanaugh, J. L. (2011). How nonlinear is the creep deformation of polar ice? A new field assessment. *Geology*, *39*, 1027–1030. https://doi.org/10.1130/G32259.1

Dahl-Jensen, D., Gundestrup, N., Gogineni, S. P., & Miller, H. (2003). Basal melt at NorthGRIP modeled from borehole, ice-core and radio-echo sounder observations. *Annals of Glaciology*, *37*, 207–212. https://doi.org/10.3189/172756403781815492

Dansgaard, W., & Johnsen, S. J. (1969). A flow model and a time scale for the ice core from Camp Century, Greenland. *Journal of Glaciology*, *8*(53), 215–233.

de Bresser, J., ter Heege, J., & Spiers, C. (2001). Grain size reduction by dynamic recrystallization: Can it result in major rheological weakening? *International Journal of Earth Sciences*, *90*, 28–45. https://doi.org/10.1007/s005310000149

de Riese, T., Bons, P. D., Gomez-Rivas, E., Griera, A., Llorens, M.-G., & Ran, H. (2018). Shear localisation in homogeneous, mechanically anisotropic materials. *Geophysical Research Abstracts*, *20*, EGU2018–EGU11875.

Durham, W. B., Heard, H. C., & Kirby, S. H. (1983). Experimental deformation of poly-crystalline H_2O ice at high pressure and low temperature: Preliminary results. *Journal of Geophysical Research*, *88*, B377–B392. https://doi.org/10.1029/JB088iS01p0B377

Fahnestock, M., Abdalati, W., Joughin, I., Brozena, J., & Gogineni, P. (2001). High geothermal heat flow, basal melt, and the origin of rapid ice flow in Central Greenland. *Science*, *294*, 2338–2342. https://doi.org/10.1126/science.1065370

Faria, S. H., Kipfstuhl, S., Azuma, N., Freitag, J., Hamann, I., Murshed, M. M., & Kuhs, W. F. (2009). The multiscale structure of Antarctica. Part I: Inland ice. *Low Temperature Science*, *68*, 39–59.

Faria, S. H., Weikusat, I., & Azuma, N. (2014). The microstructure of polar ice. Part II: State of the art. *Journal of Structural Geology*, *61*, 21–49. https://doi.org/10.1016/j.jsg.2013.11.003

Gillet-Chaulet, F., Gagliardini, O., Seddik, H., Nodet, M., Durand, G., Ritz, C., et al. (2012). Greenland ice sheet contribution to sea-level rise from a new-generation ice-sheet model. *The Cryosphere*, *6*(6), 1561–1576. https://doi.org/10.5194/tc-6-1561-2012

Gillet-Chaulet, F., Hindmarsh, R. C. A., Corr, H. F. J., King, E. C., & Jenkins, A. (2011). In-situ quantification of ice rheology and direct measurement of the Raymond Effect at Summit, Greenland using a phase-sensitive radar. *Geophysical Research Letters*, *38*, L24503. https://doi.org/10.1029/2011GL049843

Glen, J. W. (1952). Experiments on the deformation of ice. *Journal of Glaciology*, *2*, 111–114.

Glen, J. W. (1955). The creep of polycrystalline ice. *Proceedings of the Royal Society of London A: Mathematical, Physical and Engineering Sciences*, *228*(1175), 519–538. The Royal Society.

Goldsby, D. L. (2006). Superplastic flow of ice relevant to glacier and ice-sheet mechanics. In P. G. Knight (Ed.), *Glacier Science and Environmental Change* (pp. 308–314). Oxford: Blackwell.

Goldsby, D. L., & Kohlstedt, D. L. (2001). Superplastic deformation of ice: Experimental observations. *Journal of Geophysical Research*, *106*, 11,017–11,030. https://doi.org/10.1029/2000JB900336

Graham, F. S., Morlighem, M., Warner, R. C., & Treverrow, A. (2018). Implementing an empirical scalar constitutive relation for ice with flow-induced polycrystalline anisotropy in large-scale ice sheet models. *The Cryosphere*, *12*, 1047–1067. https://doi.org/10.5194/tc-12-1047-2018

Graversen, R. G., Drijfhout, S., Hazeleger, W., van de Wal, R., Bintanja, R., & Helsen, M. (2011). Greenland's contribution to global sea-level rise by the end of the 21st century. *Climate Dynamics*, *37*(7–8), 1427–1442. https://doi.org/10.1007/s00382-010-0918-8

Hewitt, I. J. (2013). Seasonal changes in ice sheet motion due to melt water lubrication. *Earth and Planetary Science Letters*, *371–372*, 16–25. https://doi.org/10.1016/j.epsl. 2013.04.022

Hooke, R. (1981). Flow law for polycrystalline ice in glaciers: Comparison of theoretical predictions, laboratory data, and field measurements. *Reviews of Geophysics and Space Physics*, *19*, 664–672. https://doi.org/10.1029/RG019i004p00664

Hutter, K. (1983). Theoretical glaciology; material science of ice and the mechanics of glaciers and ice sheets. *D. Reidel Publishing Co., Dordrecht, Terra Scientific Publishing Co*, Tokyo.

Intergovernmental Panel on Climate Change (2014). Climate Change 2014: Synthesis Report. In Core Writing Team, R. K. Pachauri, & L. A. Meyer (Eds.), *Contribution of Working Groups I, II and III to the Fifth Assessment Report of the Intergovernmental Panel on Climate Change* (p. 151). Geneva, Switzerland: IPCC.

Jansen, D., Llorens, M.-G, Westhoff, J., Steinbach, F., Kipfstuhl, S., Bons, P. D., et al. (2016). Small-scale disturbances in the stratigraphy of the NEEM ice core: Observations and numerical model simulations. *The Cryosphere*, *10*, 359–370. https://doi.org/10.5194/tc-10-359-2016

Joughin, I., Smith, B., Howat, I., & Scambos, T. (2010a). *MEaSUREs Greenland Ice velocity map from InSAR data*. Boulder, Colorado, USA: NASA DAAC at the National Snow and Ice Data Center. https://doi.org/10.5067/MEASURES/CRYOSPHERE/nsidc-0478.001

Joughin, I., Smith, B., Howat, I. M., Scambos, T., & Moon, T. (2010b). Greenland flow variability from ice-sheet-wide velocity mapping. *Journal of Glaciology*, *56*, 415–430. https://doi.org/10.3189/002214310792447734

Kamb, B., & Echelmeyer, K. A. (1986). Stress-gradient coupling in glacier flow 1. Longitudinal averaging of the influence of ice thickness and surface slope. *Journal of Glaciology*, *32*, 267–284. https://doi.org/10.3189/S0022143000015604

Karlsson, N. B., & Dahl-Jensen, D. (2015). Response of the large-scale subglacial drainage system of Northeast Greenland to surface elevation changes. *The Cryosphere*, *9*, 1465–1479. https://doi.org/10.5194/tc-9-1465-2015

Kirchner, N., Ahlkrona, J., Gowan, E. J., Lötstedt, P., Lea, J. M., Noormets, R., et al. (2016). Shallow ice approximation, second order shallow ice approximation, and full Stokes models: A discussion of their roles in palaeo-ice sheet modelling and development. *Quaternary Science Reviews*, *147*, 136–147. https://doi.org/10.1016/j.quascirev.2016.01.032

Llorens, M. G., Griera, A., Bons, P. D., Lebensohn, R. A., Evans, L. A., Jansen, D., & Weikusat, I. (2016). Full-field predictions of ice dynamic recrystallisation under simple shear conditions. *Earth and Planetary Science Letters*, *450*, 233–242. https://doi.org/10.1016/j.epsl.2016.06.045

MacGregor, J. A., Fahnestock, M. A., Catania, G. A., Aschwanden, A., Clow, G. D., Colgan, W. T., et al. (2016). A synthesis of the basal thermal state of the Greenland Ice Sheet. *Journal of Geophysical Research: Earth Surface*, *121*, 1328–1350. https://doi.org/10.1002/2015JF003803

MacGregor, J. A., Fahnestock, M. A., Catania, G. A., Paden, J. D., Gogineni, S. P., Young, S. K., et al. (2015). Radiostratigraphy and age structure of the Greenland Ice Sheet. *Journal of Geophysical Research: Earth Surface*, *120*, 212–241. https://doi.org/10.1002/2014JF003215

Paterson, W. S. B. (1991). Why ice-age ice is sometimes "soft". *Cold Regions Science and Technology*, *20*, 75–98. https://doi.org/10.1016/0165-232X(91)90058-O

Pettit, E. C., & Waddington, E. D. (2003). Ice flow at low deviatoric stress. *Journal of Glaciology*, *49*, 359–369. https://doi.org/10.3189/172756503781830584

Platt, J. P., & Behr, W. M. (2011). Grain size evolution in ductile shear zones: Implications for strain localization and the strength of the lithosphere. *Journal of Structural Geology*, *33*, 537–550. https://doi.org/10.1016/j.jsg.2011.01.018

Qi, C., Goldsby, D. L., & Prior, J. P. (2017). The down-stress transition from cluster to cone fabrics in experimentally deformed ice. *Earth and Planetary Science Letters*, *471*, 136–147. https://doi.org/10.1016/j.epsl.2017.05.008

Raymond, C. F. (1983). Deformation in the vicinity of ice divides. *Journal of Glaciology*, *29*, 357–373. https://doi.org/10.3189/S0022143000030288

Ren, D., Fu, R., Leslie, L. M., Chen, J., Wilson, C., & Karoly, D. J. (2011). The Greenland Ice Sheet response to transient climate change. *Journal of Climate*, *24*, 3469–3483. https://doi.org/10.1175/2011JCLI3708.1

Rignot, E., & Mouginot, J. (2012). Ice flow in Greenland for the International Polar Year 2008–2009. *Geophysical Research Letters*, *39*, L11501. https://doi.org/10.1029/2012GL051634

Rogozhina, I., Petrunin, A. G., Vaughan, A. P., Steinberger, B., Johnson, J. V., Kaban, M. K., et al. (2016). Melting at the base of the Greenland ice sheet explained by Iceland hotspot history. *Nature Geoscience*, *9*(5), 366–369. https://doi.org/10.1038/ngeo2689

Sergienko, O. V., Creyts, T. T., & Hindmarsh, R. C. A. (2014). Similarity of organized patterns in driving and basal stresses of Antarctic and Greenland ice sheets beneath extensive areas of basal sliding. *Geophysical Research Letters*, *41*, 3925–3932. https://doi.org/10.1002/2014GL059976

Stokes, C. R., Clark, C. D., Lian, O. B., & Tulaczyk, S. (2007). Ice stream sticky spots: A review of their identification and influence beneath contemporary and palaeo-ice streams. *Earth-Science Reviews*, *81*, 217–249. https://doi.org/10.1016/j.earscirev.2007.01.002

Treverrow, A., Budd, W., Jacka, T., & Warner, R. (2012). The tertiary creep of polycrystalline ice: Experimental evidence for stress dependent levels of strain-rate enhancement. *Journal of Glaciology*, *58*, 301–314. https://doi.org/10.3189/2012JoG11J149

Weertman, J. (1983). Creep deformation of ice. *Annual Review of Earth and Planetary Sciences*, *11*(1), 215–240.

Wolovick, M. J., Creyts, T. T., Buck, W. R., & Bell, R. E. (2014). Traveling slippery patches produce thickness-scale folds in ice sheets. *Geophysical Research Letters*, *41*, 8895–8901. https://doi.org/10.1002/2014GL062248